Preprints (www.preprints.org) | NOT PEER-REVIEWED | Posted: 17 March 2022 doi:10.20944/preprints202203.0242.v1

Article

Hyphal Fusion and Autophagy Enable Proper Conidiation and Symptom Development on Maize Leaves by *Colletotrichum graminicola*

Daniela Elisabeth Nordzieke[1,*]

[1] Georg-August-University of Göttingen, Institute of Microbiology and Genetics, Genetics of Eukaryotic Microorganisms, Grisebachstr. 8, 37077 Göttingen, Germany; dnordzi@gwdg.de
* Correspondence: dnordzi@gwdg.de

Abstract: Hyphal and germling fusion is a common phenomenon in ascomycetous fungi. Due to the formed hyphal network, this process enables coordinated development, interaction with plant hosts and efficient nutrient distribution. Recently, our lab showed a positive correlation of germling fusion with the formation of penetrating hyphopodia on maize leaves outgoing from *Colletotrichum graminicola* oval conidia. To investigate the probable interconnectivity of these processes, we have generated a deletion mutant in *Cgso*, which homologs are essential for cellular fusion in other fungal species. Indeed, plant infection studies combined with microscopy revealed a significant decrease in symptom development of the ΔCgso mutant on maize leaves. However, hyphopodia development was not affected, indicating that both processes are not directly connected. Instead, we were able to link the decreased symptom development to a reduced formation of acervuli, asexual fruiting bodies of *C. graminicola*, which give rise to falcate conidia. Monitoring of a fluorescent labelled autophagy marker eGFP-CgAtg8 revealed a high autophagy activity in hyphae surrounding acervuli. Since the ΔCgso mutant shows no hyphal fusions at these sites, we conclude that efficient nutrient transport of degraded cellular material by hyphal fusions enables proper acervuli maturation and symptom development on leaves.

Keywords: *Colletotrichum graminicola*; oval conidia; falcate conidia; germling fusion; conidiation; autophagy

1. Introduction

Colletotrichum graminicola (Ces.) G.W. Wils., originally provided by R. L. Nicholson, Purdue University, IN, is a hemibiotrophic plant pathogen. It belongs to the globally distributed genus *Colletotrichum* with about 14 species complexes consisting of a total of 250 species [1,2]. Since the members of the genus are able to infect virtually every plant and cause substantial losses on fruits, vegetables and cereals, this group ranks among the Top 10 of important plant pathogenic fungi [3]. *C. graminicola* belongs to the *graminicola-caudatum* complex, which is specialized on the infection of a wide variety of grasses, including important crops like maize and sorghum [1,4,5]. This fungus causes the disease corn anthracnose on several *Zea mays* tissues like leaves (anthracnose leaf blight, ALB), stems (anthracnose stalk rot, ASR), as well as roots and is able to cause systemic plant infection [6,7]. Combined with a high epidemic spreading potential, this pathogen is estimated to cause crop losses up to 40% per field, corresponding to 1 billion dollars/year (USA) [8,9]. Responsible for *Z. mays* infection are two morphological distinct asexual spores, oval and falcate conidia.

Falcate conidia are sickle-shaped spores formed on infected leaves by short conidiophores in asexual fruiting bodies, the acervuli [10,11]. Further typical structures in acervuli are setae, which are spike-like, highly melanized hyphae. An early study showed that setae formation is correlated to humidity [12], implying a role in moistening of acervuli

© 2022 by the author(s). Distributed under a Creative Commons CC BY license.

Preprints (www.preprints.org) | NOT PEER-REVIEWED | Posted: 17 March 2022 doi:10.20944/preprints202203.0242.v1

and probably disease spreading. To prevent germination of falcate conidia directly in their formation locus, these spores secrete mycosporines, potent self-inhibitors of germination [13,14]. In contrast, oval conidia are absent from acervuli but constricted from short hyphae during colonization and serve probably the distribution within the host plant [11,15]. Intriguingly, these conidia lack the dormant phase of falcate conidia, but germinate readily also under nutrient starvation and high spore densities, conditions which prevent the germination of falcate conidia [14]. Besides germination, nutrient starvation promotes the formation of a germling network by conidial anastomosis tubes (CATs) among oval spores, a process so far not observed for falcate conidia [14]. Furthermore, only germlings derived from oval conidia are attracted by a gradient of glucose, indicating differences in signal perception processes as well [16].

Germling fusion by the formation of CATs is a common process in ascomycetous fungi. After its first description for *Colletotrichum lindemuthianum* by Roca in 2003, this spore-density dependent process was described so far in numerous fungal species [17]. Overall, this fusion process can be divided into three sub-processes, i) the recognition of a probable fusion partner (CAT induction), ii) the directed, alternating growth towards the fusion partner (CAT homing), and iii) contacting with the counterpart, followed by pore formation and merging (CAT fusion) [18]. All of these three steps are regulated by a specific set of proteins and include Mitogen Activated Protein Kinase (MAPK) pathways, Ca^{2+} and ROS signaling [17,19]. Most prominent among the regulating proteins are the So and MAK-2 proteins firstly described in *Neurospora crassa* [20,21]. Both proteins are recruited in an oscillatory manner to the fungal tip during the chemotropic homing, a process which is therefore translated as alternating 'speaking and listening' [17,21,22]. As research in the last years showed, both proteins are part of two different MAPK cascades in fungi, the pheromone response pathway (MAK-2) and the cell wall integrity pathway (CWI) in which So serves as scaffolding protein [21,23]. Based on experiments with a *so* deletion strain in *N. crassa*, it was hypothesized that the corresponding protein is crucial for signal secretion [17,19]. As several studies indicate, the fusion signal might be not species specific since it can be sensed by several, if not all, fungal ascomycetes. For example, inter-species formation of germling fusion was shown to promote genetic variability in several *Colletotrichum* species [24,25].

In a recent study, we have shown that the ability to form germling fusions by oval conidia has severe consequences for the leaf infection strategy. In contrast to falcate conidia, which form appressoria on short germ tubes followed by rapid penetration of the plant host, a high spore density is a prerequisite for oval conidia infection [14]. Under these conditions, CAT and hyphopodia formation are induced on the maize leaf, indicating a probable interconnectivity of both processes. To prove or disprove this hypothesis, we generated a targeted deletion mutant in *Cgso.* Indeed, we observed a strong reduction of leaf symptom development, which was, however, not restricted to oval conidia infection. As detailed analyses of early fungal infections showed, ΔCgso still develops hyphopodia in a spore density-dependent manner, although germling fusions are absent in this mutant. These results indicate that both processes, although relying on colony density, are not connected. Instead, we have identified a severe defect in acervuli maturation as cause for the reduced symptom development. Analyses of acervuli-forming regions revealed a high number of *C. graminicola* wildtype hyphae are either vacuolized or empty, but remain in contact with the living mycelium by hyphal fusions. Localization studies using the green-fluorescent autophagy marker protein eGFP-CgAtg8 showed that *C. graminicola* actively degrades its own cellular material in acervulus-forming regions, which then serves the nutrition of the developing fruiting bodies. In such a setup, the developmental defect in a ΔCgso strain might be caused by an abolished distribution of degraded cellular material resulting in insufficient acervulus nutrition.

Preprints (www.preprints.org) | NOT PEER-REVIEWED | Posted: 17 March 2022 doi:10.20944/preprints202203.0242.v1

2. Materials and Methods

2.1. Strains, media and growth conditions

The wildtype strain CgM2 (M1.001) of *C. graminicola* (Ces.) G.W.Wilson was used in this study [2,26]. For the generation of falcate conidia, *C. graminicola* was grown on oat meal agar (OMA) for 14-21 d at 23°C [14]. Oval conidia as basis for *C. graminicola* transformation and experimental procedures were obtained in shaking cultures in liquid complete medium with 0.5 M of sucrose (CMS) for two days (80 rpm, 23°C) followed by 5-8 days incubation in darkness [14]. Microscopy of developing acervuli was performed from cultures grown on microscopic slides coated with a reduced OMA medium (OMA_{red}). For the preparation of OMA_{red}, 20 g of oat meal (Oat meal Feinblatt, Alnatura) were boiled in 500 ml of A. dest for 20 min. After cooling, the watery part of the oat meal suspension was filtrated through a cloth (Miracloth, EMD Millipore Corp., Billerica, MA, USA), filled with A. dest up to 1 l and supplemented with 15 g of Agar-agar per liter. For selection of transformants, complete medium (CM) containing hygromycin B (500 µg/ml, hyg; EMD Millipore Corp., Billerica, MA, USA), nourseothricin-dihydrogen sulphate (150 µg/ml, nat; Jena Bioscience GmBH, Jena, Germany) or geneticin disulphate (G418, 400 µg/ml, gen; Carl Roth GmbH + Co. KG, Karlsruhe, Germany) were used. For cloning, *Escherichia coli* strain MACH1 (Thermo Fisher Scientific, C862003, Waltham, USA) was used in standard culture conditions [27].

2.2. Generation of plasmids

Plasmids were generated via the NEBuilder HiFi DNA Assembly Cloning Kit (New England Biolabs) according to the instruction manual. Information about all primer sequences, plasmids and strains are provided in Table S1-S3.

For the generation of the *Cgso* (GLRG_01399) deletion construct, three fragments were amplified for the assembly with pJet1.2 (Thermo Fisher Scientific) using the NEBuilder HiFi DNA Assembly Cloning Kit (New England Biolabs). Approximately 1 kb of *Cgso* 5′ and 3′ regions were amplified using the primer pairs so_P_fw/so_P_rv (1049 bp) and so_T_fw/so_T_rv (1111 bp) from CgM2 genomic DNA. Amplification of *hph* cassette mediating the resistance to hygromycin B was performed using primer pair hph-f/hph-r (1417 bp) with the plasmid pRS-hyg as template [28]. By the assembly of the three fragments with pJet1.2, the plasmid pCgso_KO was generated.

For the generation of the plasmid pCgso_c_nat used for complementation of a ΔCgso null mutant, two fragments were obtained via PCR. For the amplification of *Cgso* including 5′ and 3′ regions, the primer pair so_P_comp_fw x so_T_comp_rv (59015 bp) was used. For further subcloning, *Eco*RV restriction sites were integrated in the sequences of both oligonucleotides. The *nat* cassette, mediating resistance to nourseothricin was amplified from pRS_nat [29] using the primer pair nat-1r/PtrpC_pJet (943 bp). Both fragments were assembled with pJet using NEBuilder HiFi DNA Assembly Cloning Kit (New England Biolabs). Outgoing from pCgso_c_nat, the plasmid pJet_nat harboring the *nat* resistance cassette was generated via hydrolysis with *Eco*RV and subsequent ligation with the plasmid backbone.

To allow for the visualization of autophagy in *C. graminicola*, the plasmid peGFP-Cgatg8_gen was constructed. Three fragments were amplified using PCR. The *Cgatg8* 5′ region (Atg8_P_fw/Atg8_P_rv = 1024 bp) and the *Cgatg8* gene (GLRG_08058) including 3′ terminator region (Atg8_wostart_fw/Atg8_T_rv = 1646 bp) were generated from CgM2 gDNA, eGFP was amplified from plasmid p1783-1 [30] using the oligonucleotides GFP-f/GFP-r = 716 bp.

Primers were synthesized by Sigma-Aldrich Chemie GmbH (Taufkirchen, Germany). DNA sequencing of the plasmids was performed by Microsynth Seqlab GmbH (Göttingen, Germany).

Preprints (www.preprints.org) | NOT PEER-REVIEWED | Posted: 17 March 2022 doi:10.20944/preprints202203.0242.v1

2.3. Transformation of C. graminicola strains

Prior to transformation in CgM2, all plasmids were linearized (pCgso_KO: *Hind*III and *Not*I, pCgso_c_nat: *Pvu*I, peGFP-Cgatg8_gen: *Mun*I). Protoplasts were obtained from oval conidia of wildtype CgM2 (transformation of pCgso_KO and peGFP-Cgatg8) or ΔCgso (transformation of pCgso_c_nat) by cell wall digestion using lysis enzyme of *Trichoderma harzianum* as described previously [31]. To obtain homokaryotic transformants, colonies that had developed on CM plates supplemented with 500 µg/ml hygromycin B (pCgso_KO), 150 µg/ml nourseothricin-dihydrogen sulphate (pCgso_c_nat) 400 µg/ml geneticin disulphate (peGFP-Cgatg8_gen), were allowed to conidiate on OMA. After single spore isolation using the generated falcate conidia, resistant transformants verified by PCR and Southern Blotting.

To identify *Cgso* null mutant strains, genomic DNA (gDNA) of the transformants growing on CM plates supplemented with 500 µg/ml hygromycin B was isolated and initially analyzed by PCR using the primer pair so_P_fw/so_T_rv (CgM2: 5.9 kb, ΔCgso: 3.5 kb). Prior to verification of ΔCgso via Southern Blot hybridization, gDNA was hydrolyzed with *Sac*I, resulting in specific bands after probe hybridization of 1303 bp (CgM2) and 6242 bp (ΔCgso). A *Cgso*-specific probe was obtained with the primer combination so_T_fw/so_T_rv (Figure S1).

To confirm successful ectopic integration of pCgso_c_nat and peGFP-Cgatg8_gen, PCRs were performed with the primer pairs so_seq_fw2/so_seq_rv2 and GFP-r/Atg8_P_fw, respectively.

2.4. Growth and conidiation analyses

To access the growth rates and conidiation of *C. graminicola* CgM2, ΔCgso and ΔCgso_c, precultures were grown on CM with the appropriate antibiotics. For growth rate analyses, fresh CM plates were inoculated with a defined mycelial plug (Ø 9 mm) from the corresponding preculture plate an incubated at 23°C. At days 3-7 after inoculation, colony size was recorded using a scanner (Epson Perfection V600 Photo, Epson, Tokyo, Japan) every 24 h. From the obtained pictures, the growth area of the single colonies derived from at least six biological replicates was determined using Fiji (mark area→measure; [32]). From these, growth rates were calculated as the difference of the growth area of two subsequent days. To access morphological differences and conidiation of falcate conidia, CgM2, ΔCgso and ΔCgso_c were inoculated on OMA and CM plates outgoing from the obtained precultures with a defined mycelial plug (Ø 9 mm) and incubated at 23°C for 21 d. Prior to harvest of falcate conidia, pictures of the overgrown plates were taken as described above. Harvest of falcate conidia was done using 0.02% Tween 20. After centrifugation for 10 min, 4000 rpm, the supernatant was discarded and the falcate conidia resuspended with 3 ml of 0.01% of Tween 20. From these solutions, numbers of spores and final volume was determined, serving as the basis for the calculation of total falcate conidia generated per plate in a total of six experiments. Conidiation of oval conidia was determined in flasks containing liquid 100 ml CMS cultures inoculated with five mycelial plugs each (Ø 9 mm) derived from the CM precultures. After shaking for 2 d at 80 rpm, cultures were further incubated for 6 d in darkness (23°C). To separate oval conidia from mycelia, the cultures were filtered through a sterile cloth (Miracloth, EMD Millipore Corp., Billerica, MA, USA). The flow through was centrifuged for 10 min, 4000 rpm and the pellet resuspended in 500 µl of A. dest. From these solutions, the numbers of spores and the final volume was determined, serving as the basis for the calculation of total oval conidia generated per flask in a total of six independent experiments.

2.5. Quantification of conidial anastomosis tube (CAT) formation

For the examination of germling fusion formation, 50 µl of c=5 × 10^7 ml^{-1} of oval conidia were spread on nutrient poor water agar (1% Serva Agar, 1% agarose, 25 mM $NaNO_3$) and incubated at 23°C for 17h as described previously [14]. For each of the three

Preprints (www.preprints.org) | NOT PEER-REVIEWED | Posted: 17 March 2022 doi:10.20944/preprints202203.0242.v1

independent replicates, at least 100 conidia were examined for fusion with other conidia or hyphae.

2.6. Acervuli development

For the analysis of acervuli development, CgM2, ΔCgso, ΔCgso_c, and CgM2::eGFP-Cgatg8 precultures were grown on CM with the appropriate antibiotics. From these, mycelial plugs were transferred to microscopic slides overlayed with OMA_{red} and incubated for 5 d at 23°C. From the strains CgM2, ΔCgso, ΔCgso_c pictures were taken from hyphae which showed the starting of acervulus development, indicated by a single seta. Depending on the orientation of the hypha, a length of 266.19-356.29 µm was evaluated for the presence of hyphal fusions, empty or vacuolized hyphal compartments for a total of 30 hyphae of all strains. Different layers of developing avervuli were recorded in a fixed distance of 1 µm and processed with Fiji (Image→Stacks→Images to Stacks; Image→Stacks→Z-Projection (sum slices); [32]).

2.7. Microscopy

Microscopic documentation was performed with the AxioImager M1 microscope (Zeiss, Jena, Germany) with differential interference contrast (DIC). Image capturing was performed with a Photometrix CoolSNAP HQ camera (Roper Scientific, Photometrics, Tucson, AZ, USA). Images were processed using ZEISS ZEN Digital Imaging (version 2.3; Zeiss). For visualization of expressed green-fluorescent *CgAtg8*, Chroma filter set 49,002 (exciter ET470/40x, ET525/50m, beamsplitter T495lpxr) was used. For each experiment, at least three biological replicates were analyzed.

2.8. Plant infection assays

The *Zea mays* cultivar Mikado (KWS SAAT SE, Einbeck, Germany) was grown as described previously at a day-night cycle (12 h light : 12 h dark, 26°C : 18°C) in a PK 520 WLED plant chamber (Poly Klima Climatic Growth System, Freising, Germany) [14]. To determine the formation of infection structures and symptom development after 1 or 5 dpi, secondary leaves from 16 days old maize plants were cut from the plant and fixed on top of a wet blotting paper (BF2 580x600 mm, Sartorius, Germany). 10 µl drops of conidia suspension in 0.01% Tween 20 solutions in final inocula of 10^3 and 10^2 were applied onto leaves and incubated at 22°C. To examine the early events of plant infection, the experiment was stopped 24 h after inoculation and the leaves bleached in 100% ethanol as described previously [14]. The rates of infection structures and germling fusion per conidium were assessed for at least three different infection areas. Different layers of infected leaves were recorded in a fixed distance of 1 µm and processed with Fiji (Image→Stacks→Images to Stacks; Image→Stacks→Z-Projection (sum slices); [32]). Symptom development of single inoculation spots was rated at 5 dpi using an index ranking from 1 (no symptoms), 2 (minor symptoms), 3 (symptoms) to 4 (severe symptoms) [14] for at least 40 individual spots. As negative controls, mock infections were inoculated with 10 µl of 0.01% Tween 20. To test for the penetration ability of *C. graminicola* strains, a defined inoculum (Ø 9 mm) from a preculture on CM was transferred to a single cellophane sheet (Cellophane Sheets II, 140 × 133 mm, SERVA Electrophoresis GmbH, Heidelberg, Germany) topping OMA. After incubation for 3 d at 23°C, the cellophane was removed and further incubated for 4 d, followed by examination for colony outgrowth. All experiments were performed at least in three independent replicates.

2.9. Statistics

For all experiments presented in this study, the t-test for unequal variances, also referred to as Welch-test [33], was used for all experiments displayed.

Preprints (www.preprints.org) | NOT PEER-REVIEWED | Posted: 17 March 2022 doi:10.20944/preprints202203.0242.v1

3. Results

3.1. A Cgso deletion mutant is drastically reduced in conidiation of falcate spores

In a recent study, we have found a correlation in C. graminicola oval conidia between the formation of a germling network by fusions and symptom development on leaves. As infection assays revealed, high spore densities induced the formation of CATs and penetrating hyphopodia out of a hyphal network. In contrast, low spore densities diminished significantly germling fusion and the number of hyphopodia formed per spore [14]. From these results, we deduced that hyphal network formation by oval conidia might be a prerequisite for the efficient formation of penetration structures and symptom development. To follow this hypothesis, we performed a BLAST search and identified a C. graminicola gene homologous to so in N. crassa, a key player in the fusion of fungal cells in that fungus [21]. We then generated a null mutant of the identified gene Cgso (GLRG_01399) by replacing the native gene with a hph cassette, mediating resistance to hygromycin B (Figure S1). Already during the verification process, we observed a strong phenotype of ΔCgso in conditions promoting the conidiation of falcate conidia. In contrast to the wildtype strain, which shows massive falcate conidia generation after 21 d of growth on OMA, ΔCgso deletion mutants show formation of arial mycelia, embedding a more than 100 x reduced number of falcate conidia. This phenotype is reversed in a ΔCgso strain with a re-integrated Cgso gene (Figure 1). To test whether the reduced conidiation of ΔCgso might be caused by a vegetative growth defect, growth rates of all three strains were compared. However, no substantial differences were be observed (Figure S2). We further analyzed whether the Cgso deletion affects conidiation processes of C. graminicola in general, and thus compared oval conidia generation in wildtype and the deletion strain. Strikingly, we have found no significant differences, indicating a spore-type specific conidiation defect (Figure S3)

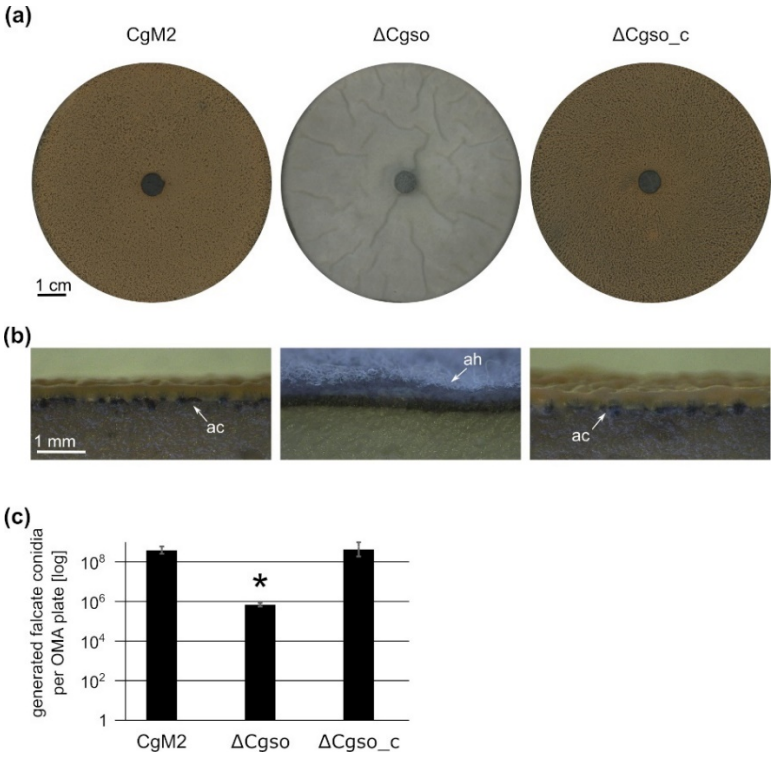

Figure 1. Generation of falcate conidia in *C. graminicola* strains. *C. graminicola* CgM2 (wildtype), ΔCgso deletion strain as well as ΔCgso with a re-integrated Cgso gene including native 5' and 3' regions (ΔCgso_c) were incubated for 21 d on oatmeal agar (OMA) plates at 23°C. (**a**) Plate overview, scale bar = 1 cm; (**b**) cross section, scale bar = 1 mm, ac = acervuli, ah = aerial hyphae; (**c**) Quantification of falcate conidia per plate. Values are depicted in a logarithmic scale, error bars represent SD calculated from 6 experiments, *, $p < 0.05$.

Preprints (www.preprints.org) | NOT PEER-REVIEWED | Posted: 17 March 2022 doi:10.20944/preprints202203.0242.v1

ΔCgso is defective in germling fusions and shows reduced symptom development on Z. mays leaves

Since homologous so deletion mutants in other fungi show a complete loss of germling and hyphal fusion ability [17]. As our results show, C. graminicola is no exception in this regard: the oval conidia-specific CAT fusion process is completely absent from ΔCgso, but restored by re-integration of the Cgso gene (Figure S4). To test whether the absence of germling fusion ability interferes with symptom development of oval conidia on leaves, infection analyses were performed. We inoculated each leaf with five droplets per leave containing high (10^3) and low (10^2) inocula of either falcate or oval conidia, resulting in different spore densities on the inoculation spots (Figure S5). As depicted in Figure 2, CgM2 inoculation result in the development of evenly distributed acervuli 5 dpi which is strongest on the inoculation spot itself and spreads to the surroundings. After the same time, ΔCgso inoculation spots remain mostly empty of developing acervuli. Instead, some acervuli form along vascular bundles outside of the inoculation spot. Interestingly, this effect is independent on the spore inoculum and was observed in oval as well as falcate conidia infections.

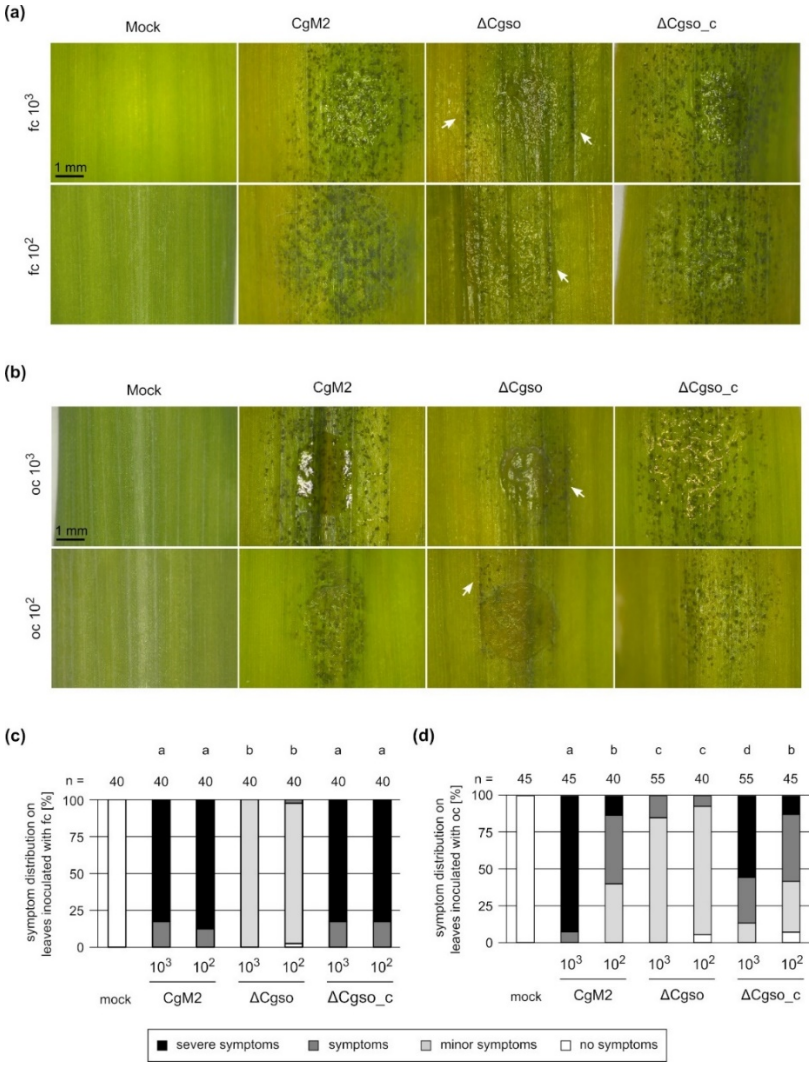

Figure 2. *Zea mays* leaf infection. Second leaves of 16 d old *Z. mays* plants (cv Mikado) were inoculated with droplets *C. graminicola* conidia containing 10^3 or 10^2 conidia. (**a-b**) Typical appearance of symptoms on intact leaves is depicted after incubation with falcate (fc, (**a**)) or oval (oc, (**b**)) conidia for 5 d. Arrows indicate development of acervuli along vascular bundles, scale bar = 1 mm; (**c-d**) Symptom development caused by falcate (**c**) or oval (**d**) conidia was rated using an established category system [14], n = number of experiments; a, b, c, d, $p < 0.05$.

Preprints (www.preprints.org) | NOT PEER-REVIEWED | Posted: 17 March 2022 doi:10.20944/preprints202203.0242.v1

In the following, a detailed comparison of symptom development was done by the application of our standardized rating system of individual inoculation spots [14]. For falcate conidia infections, predominantly severe symptoms are developed in CgM2 as well as in ΔCgso_c for both high and low spore inocula. In contrast, only minor symptoms were detected in response to inoculation with ΔCgso. In leaf infection assays with oval conidia, we verified previous results of our lab showing a significant reduced symptom development when low spore densities are present (Figure 2). However, in the ΔCgso infection experiments this interdependence is reversed and minor symptoms dominate for both spore concentrations tested.

3.2. A defective germling fusion process does not affect hyphopodia formation by oval conidia

To explain the observed symptom development 5 dpi, further leaf infection experiments were conducted which were aborted 1 dpi. After bleaching of the corresponding leaves, microscopic observations of the first steps of the leaf infection process was possible (Figure 3). Here, oval conidia of both CgM2 wildtype and ΔCgso_c complementation strain showed frequent germling fusion and hyphopodia formation in spots inoculated with high spore densities. However, on leaves inoculated with ΔCgso oval conidia, no germling fusion events were observed. Intriguingly, the formation rate of hyphopodia was comparable to wildtype and complementation strain (Figure 3).

Comparing these results to our previous observations of symptom development 5 dpi, the differences in hyphopodia formation rate in CgM2 and ΔCgso_c is very well reflected by spore inocula-dependent symptom development (Figure 2). However, the symptom development of ΔCgso does not follow this line, indicating a severe defect in the mutant's development in planta. To rule out a probable penetration defect of ΔCgso, a qualitative penetration assay was performed. Here, in the total of nine biological replicates, no differences in between all three strains tested was observed.

3.3. Autophagy-degraded cellular material serves for the nutrition of acervuli

Since we observed a reduced number of acervuli on cultivation media as well as on infected leaves (Figure 1, Figure 2), we examined this process after 5 d of inoculation on a reduced OMA medium (OMA_{red}). As it is depicted in Figure 4 A, the overall density of setae, typical markers of developing acervuli, is highly reduced in ΔCgso. Additionally, we observed a high number of aerial hyphae in ΔCgso, which are formed, like setae, from dark-pigmented hyphal fragments. To analyze acervuli development in detail, we had a look at young developing acervuli, indicated by single setae (Figure 4 B). In all strains, we observed several empty or highly vacuolized hyphal compartments, separated by septae. Intriguingly, in ΔCgso these parts seem to separate the young acervuli from living fungal tissue. In CgM2 and ΔCgso_c, however, we monitored frequent fusion of neighboring hyphae, connecting again the asexual fruiting bodies with living fungal cells. To access whether or not these processes are limited to hyphal regions with developing acervuli, we have quantified the number of empty and vacuolized hyphal compartments as well as hyphal fusion events in acervuli and non-acervuli regions (Figure 4, Figure S6). However, no differences were observed, indicating that these are general processes taking place in a C. graminicola colony of that age.

Preprints (www.preprints.org) | NOT PEER-REVIEWED | Posted: 17 March 2022 doi:10.20944/preprints202203.0242.v1

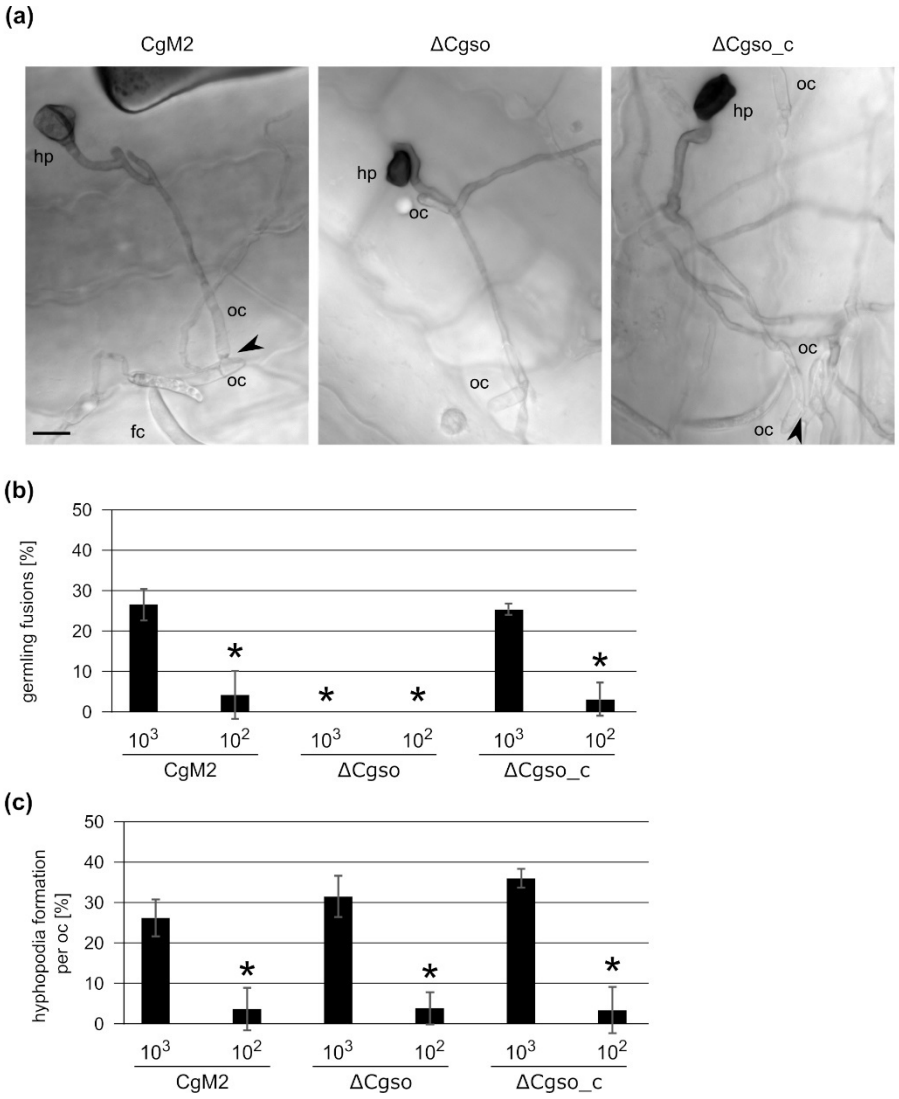

Figure 3. Hyphopodia and cellular fusion formation by oval conidia-derived germlings. Inoculation of secondary leaves obtained from 16 d old *Zea mays* (cv Micado) plants with 10^3 and 10^2 oval conidia of the depicted strains. 1 dpi, the infection process was stopped. Leaves were parted in four and decolorized in 100% EtOH for 3 d. (**a**) Typical representation of colony and infection structure development with an inoculum of 10^3 at 1 dpi, hyphal fusions are indicated with black arrow heads, oc = oval conidia, fc = falcate conidia, hp = hyphopodia, scale bar = 10 µm; (**b-c**) Quantification of cellular fusions (**b**) or hyphopdia (**c**) formed by germlings derived from oval conidia in one inoculation spot. Error bars represent SD calculated from ≥ 3 experiments, *, $p < 0.05$.

Having in mind the results of our leaf infection experiments in which acervuli of ΔCgso only formed along vascular bundles, we speculated about a probable interconnection of coordinated cellular degradation and nutrition of the developing acervuli. In such a setup, the formed hyphal fusion bridges of CgM2 and ΔCgso_c might be crucial to transport the degraded cellular material to the nutrient sink. In strains defective of cellular fusion, the nutrition of acervuli would stop after an early time point, resulting in a reduced number of falcate conidia. To verify this hypothesis, we grew all three strains on complex medium, which is promoting vegetative growth but no acervuli development. Intriguingly, quantification of falcate conidia from these plates showed no significant differences in between all three strains, indicating an early abortion of acervuli development of the ΔCgso mutant in planta due to nutrient limitations (Figure 5, Figure S7).

Preprints (www.preprints.org) | NOT PEER-REVIEWED | Posted: 17 March 2022 doi:10.20944/preprints202203.0242.v1

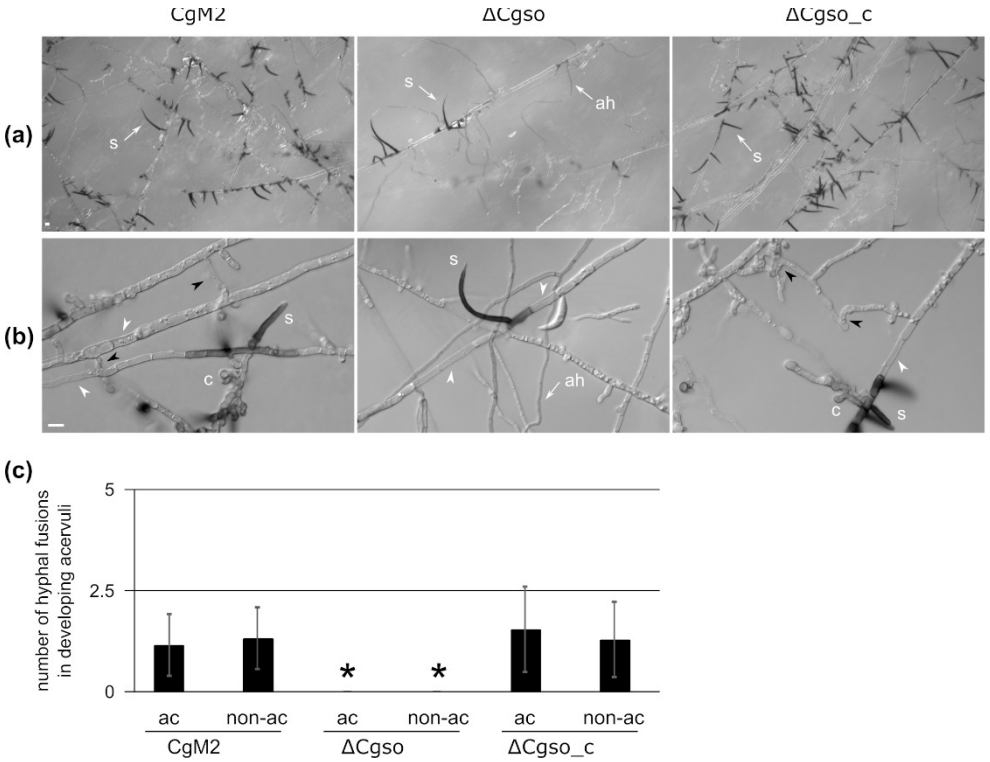

Figure 4. Development of young acervuli in a *Cgso* deletion strain. *C. graminicola* CgM2 (wildtype), ΔCgso deletion strain as well as the corresponding complementation strain ΔCgso_c were analyzed for the development of asexual fruiting bodies, the acervuli. Depicted strains were inoculated on microscopic slides covered with reduced oat meal agar (OMA_{red}) for 5 d, 23°C. ah = aerial hyphae, s = setae, hyphal fusions are indicated with black arrow heads, empty hyphal compartments with white arrow heads, scale bar = 10 µm. (**a**) Overview of acervuli forming regions; (**b**) Z-projections of stack images of hyphae with developing setae and conidiophores (levels of 1 µm); (**c**) Total numbers of hyphal fusions on hyphae, which show (ac) or do not show (non-ac) developing acervuli. Error bars represent SD calculated from 30 experiments, *, $p < 0.05$.

Due to the prominent empty or vacuolized hyphal compartments at developing acervuli, we speculated about a controlled degradation process at these sites. Autophagy is an intracellular vacuolar degradation process in eukaryotes, which regulates starvation adaptation as well as developmental processes [34]. To test whether autophagy takes place at sites of developing acervuli, a strain expressing green-fluorescent CgAtg8 was generated. Since Atg8 proteins in other fungi can be localized in small autophagosomes as well as in larger vacuoles depending on the age of the fungal hyphae [35], we first checked the overall localization patterns in CgM2::eGFP-Cgatg8. As depicted in Figure S8, expression of eGFP-CgAtg8 results in green fluorescent autophagosomes in young fungal filaments, whereas in older hyphae, we monitored a strong accumulation of the signal in vacuoles. Monitoring of the same strain after 5 d growth on OMA_{red}, we observed a bright fluorescence in hyphae both forming and surrounding the acervulus. The fluorescent signal filled large parts of the hyphal segments which we declared as strongly vacuolized in our quantification analyses (Figure 4, Figure 5 B), indicating that the autophagy degradation process is highly accelerated compared to normal aging hyphae (Figure S8). Interestingly, the formed hyphal fusion bridges showed a strong green fluorescent signal as well, supporting the hypothesis that these are required for successful transport of degraded cellular material for acervulus maturation.

Preprints (www.preprints.org) | NOT PEER-REVIEWED | Posted: 17 March 2022 doi:10.20944/preprints202203.0242.v1

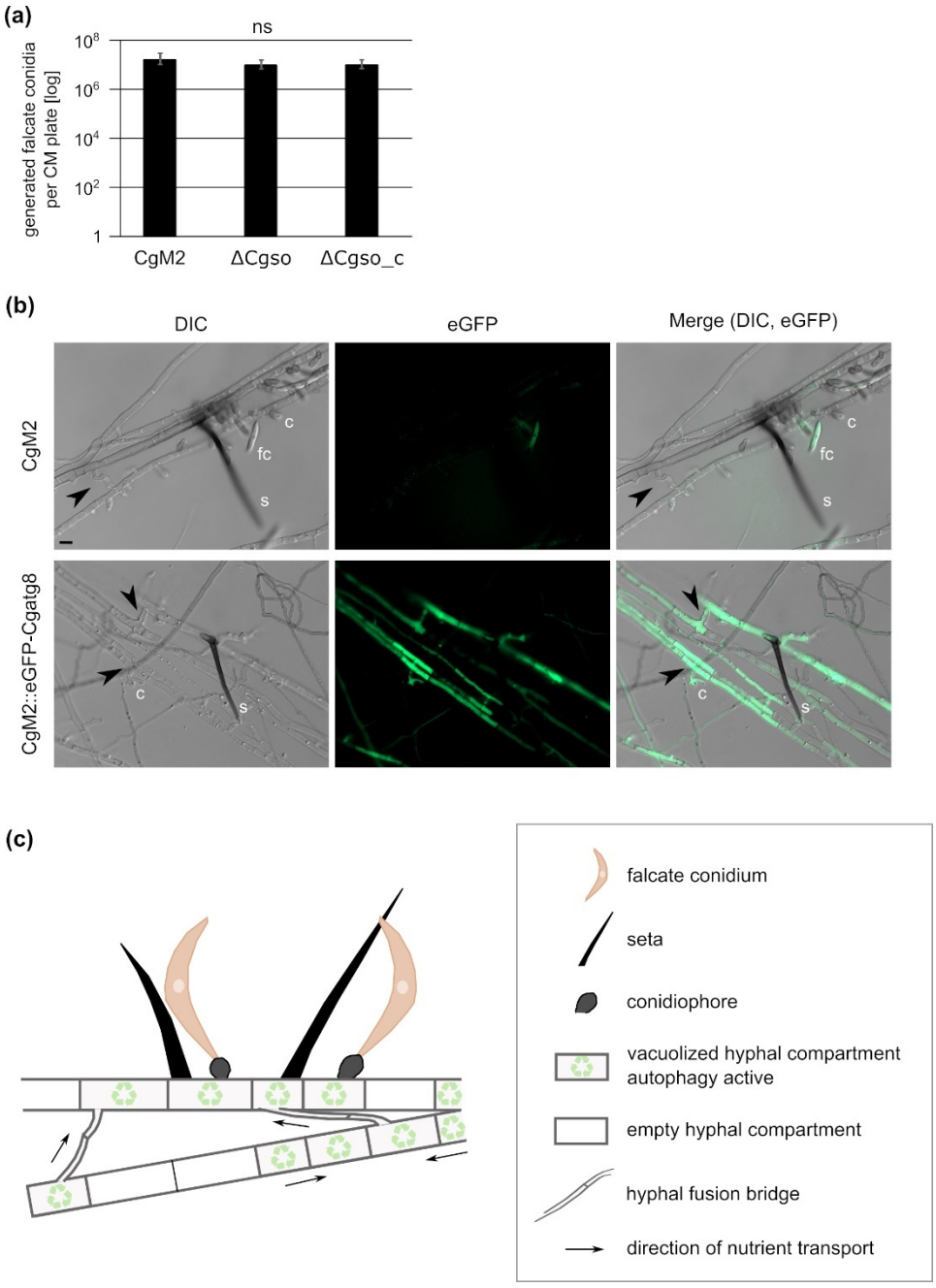

Figure 5. Autophagy in developing acervuli and model. (**a**) Quantification of falcate conidia after growth on complex medium (CM) for 21 d, 23°C. Values are depicted in a logarithmic scale, error bars represent SD calculated from 6 experiments, ns, $p > 0.05$; (**b**) *C. graminicola* wildtype strain CgM2 and CgM2::eGFP-Cgatg8 expressing green fluorescent autophagy marker CgAtg8 were inoculated on microscopic slides covered with reduced oat meal agar (OMA_{red}) for 5 d, 23°C. Selected layers from acervuli recordings with a fixed distance of 1 µm are depicted for each strain, s = setae, c = conidiophores, fc = falcate conidia, hyphal fusions are indicated with black arrow heads, scale bar = 10 µm; (**c**) Optimized distribution of autophagy-recycled cellular components by hyphal fusion bridges allows for proper acervulus maturation and falcate conidia production in *C. graminicola*.

4. Discussion

4.1. An unknown quorum sensing mechanism regulates hyphopodia formation out of oval conidia

As our investigations show, different developmental processes are induced in *C. graminicola* depending on the amount of spores applied, thus showing typical characteristics of quorum sensing (QS) processes. QS was first discovered in the 1960s in gram

Preprints (www.preprints.org) | NOT PEER-REVIEWED | Posted: 17 March 2022 doi:10.20944/preprints202203.0242.v1

positive bacteria [36,37]. In this process, small signaling molecules (quorum sensing molecules, QSM) are secreted, which are able to shape the behavior of the sensing microorganisms [38]. Since then, QS was discovered for multiple bacteria but also fungal species and is nowadays accepted as central mechanism of inter-kingdom communication [39,40]. In *C. graminicola*, two QS dependent processes are described. Falcate conidia secrete mycosporines as germination inhibitors when present in high spore numbers, like acervuli [13,14]. Also the formation of germling fusions is dependent of spore densities, as it is documented for *C. graminicola* as well as several other fungi [14,24,41-43]. In an earlier study, we have further observed a positive correlation of the formation of penetrating hyphopodia by oval conidia and the germling fusion process on leaves, indicating that also the pathogenicity program of oval conidia is dependent on the spore concentration [14]. In this current study, we thus have generated and analyzed a deletion mutant in the *C. graminicola so* gene, essential gene for cellular fusion in other fungi. As we have found out by detailed leaf microscopy, hyphopodia formation remains dependent on conidia density, independent of the ability of the investigated strain to perform fusion or not (Figure 3). These results indicate that a third QS process regulates the formation of penetration structures from oval conidia. Such involvement of QS in host infection was shown for many pathogenic bacteria. In those processes, QS enables the synchronized expression of virulence factors, enabling the microbe to overcome the host´s defense mechanisms [44]. Also for the fungus *Colletotrichum coccodes*, a positive correlation of penetration structure formation and inoculum size was shown [45]. One possible explanation of this phenomenon would be spore-density dependent secretion of germination enhancers, which would indirectly affect hyphopodia formation. In a recent study, positive and negative germination regulation of the tomato wilt fungus *Fusarium oxysporum* f. sp. *lycopersici* by pheromone signaling was shown. Intriguingly, the α-pheromone interaction with the Ste2 receptor leads to repression of conidial germination, while the interaction of the a-pheromone with the Ste3 receptor relieves repression in a cell-density-dependent manner [46]. However, we observed no density-dependent differences in germination patterns in *C. graminicola* oval conidia [14], indicating that the determining QS mechanism might be specific for hyphopodia development.

4.2. Coordinated nutrient recycling and distribution is the basis for acervulus maturation

Proper development of distinct morphological structures in fungi like appressoria, sexual fruiting bodies, and the formation of conidiophores require the mobilization and translocation of nutrients [47]. Seeking for explanations for the drastically reduced falcate conidia production and decreased amounts of acervuli formed on infected leaves of the ΔCgso mutant strain, we monitored the developing conidiation sites in detail (Figure 4). There we observed a high number of empty or heavily vacuolized compartments, which are bridged by hyphal fusions in the CgM2 wildtype strain and the ΔCgso complementing strain. From these observations we deduced that probably autophagy, a controlled degradation process in eukaryotic organisms, takes place at developing acervuli.

In general, one can distinguish between three autophagy types, microautophagy, macroautophagy and chaperon-mediated autophagy. Fungal macroautophagy describes the formation of a double-membrane vesicle, the autophagosome, outgoing from the phagophore assembly site (PAS) [48-50]. Within the autophagosome, a portion of cytoplasm is engulfed containing excessive or defective proteins and organelles [49,51]. These autophagosomes fuse with vacuoles, resulting in the degradation of the inner autophagosomal membrane as well as its cargo by hydrolases [52,53]. Responsible for the correct assembly of the PAS, binding of cargo, autophagosome fusion with vacuoles and finally its degradation, are autophagy-related (Atg) proteins. In yeast, 36 Atg proteins were described, of which many are conserved in all eukaryotes, including filamentous fungi [54,55]. One of these is Atg8, a ubiquitin-like protein, of which a conjugate with lipid phosphatidylethanolamine (PE) is formed to anchor the protein to the forming autophagosomal membrane at PAS. Therefore, Atg8 is a structural component of the autophagosome

Preprints (www.preprints.org) | NOT PEER-REVIEWED | Posted: 17 March 2022 doi:10.20944/preprints202203.0242.v1

and remains bound to its membrane until the degradation in the vacuole took place [56,57].

Recently, autophagy was investigated in several fungal species. Phenotypic investigations of *atg* deletion mutants revealed defects in proper sexual and asexual development, vegetative growth, resistance to various stresses (nitrogen, carbon, metal ion starvation, reactive oxygen species, osmotic stress), and pathogenicity [47,54,58,59]. Several of these processes have been linked to improper nutrition of developing structures like appressoria, sexual fruiting bodies and conidiophores due to defects in the overall autophagy process [47]. To investigate a probable role of autophagy in acervulus development, we fused green fluoresecent eGFP N-terminally to CgAtg8 and expressed the fusion protein in wildtype CgM2. Intriguingly, hyphae of the resulting strain CgM2::eGFP-Cgatg8 showed typical Atg8 localization patterns known from other fungi: dotlike autophagosomes in young hyphae and bright green vacuoles in older tissues (Figure S8, [35,60]). Furthermore, at sites of acervuli development, we monitored that complete hyphal segments shine bright green, indicating a massive turnover due to active autophagy in these regions (Figure 5). A similar pattern was shown for fluorescent-tagged Atg8 in *Magnaporthe oryzae*. In this fungus, Atg8 is brightly visible in developing conidiophores, conidia and aerial hyphae [60]. At the same time, an *Moatg8* deletion strain is heavily affected in conidiation, but also vegetative growth and virulence [61,62]. Similar defects in conidiation were observed also for homologous *atg8* deletion mutants in various other fungi like *Aspergillus ssp.*, *Colletotrichum orbiculare*, *Ustilaginoidea virens*, and *F. graminearum*, indicating a general requirement for cellular degradation for the nutrition of conidiophores [63-68]. Intriguingly, in *U. virens* the observed reduced virulence of ΔUvatg8 was explained with its decreased conidiation rate [68], similar to our observations for ΔCgso.

In the same experiments using eGFP-Cgatg8 as autophagy marker, it was obvious that within the autophagy active regions, hyphal fusions bridges form readily in wildtype and ΔCgso::Cgso strains, supporting the idea that hyphal fusions enable efficient distribution of the degraded cellular material to the point of need (Figure 5). Hyphal and germling fusion were intensively studied since their first description in 2003 in *C. lindemuthianum* by Roca and coworkers [69]. Since then, several additional defects were observed for gene deletion mutants affected in fusion processes. For example, in the coprophilous fungus *Sordaria macrospora* defects in the hyphal fusion process goes often hand in hand with an aborted sexual development [23,70-79]. From this co-occurrence of phenotypes it was deduced that the fusion process is either a prerequisite for proper sexual fusion within the maturing fruiting bodies or that the nutrition of this sexual structure is decreased. Intriguingly, there are some exceptions from this rule: deletion mutants in autophagy genes like *atg8* and *atg4* are sterile, but their ability to from fusion bridges remains intact [35,80]. It is tempting to assume that fusion formation and autophagy, despite being independent, are both dedicated to enable the same development process. Also the results of this study support such a perspective: although ΔCgso is unable to form hyphal fusions, the number of empty or vacuolized hyphal compartments at developing acervuli does not differ to the fusion competent CgM2 and ΔCgso::Cgso strains (Figure S6). This perspective might also explain the reduced symptom development on leaves (Figure 2). The wildtype CgM2 and the ΔCgso complementing strain produce acervuli predominantly at sides with a high hyphal density *in planta* within the area of the inoculation spot. In contrast, acervuli are absent from these parts in the *Cgso* null mutant, but form along vascular bundles outside the inoculation site. There, nutrient-rich phloem could further support acervuli development and thus might compensate for the defective nutrient distribution caused by the absence of hyphal fusions.

5. Conclusions

The formation of fungal networks by the fusion of hyphae and/or conidia is a typical feature of filamentous ascomycetes. Combining microscopic analyses with *Z. may* leaf infection assays, we show that hyphal fusion together with autophagy are crucial for

Preprints (www.preprints.org) | NOT PEER-REVIEWED | Posted: 17 March 2022 doi:10.20944/preprints202203.0242.v1

efficient nutrition of asexual fruiting bodies. Thus, defects in the fusion process results in a decreased conidiation of falcate conidia and reduced symptom development on leaves. Furthermore, we provided evidence that the formation of penetrating hyphopodia by *C. graminicola* oval conidia rely on an unknown quorum sensing mechanism which is independent of germling fusion formation.

Supplementary Materials: Supplementary Materials: The following supporting information can be downloaded at the website of this paper posted on Preprints.org. Figure S1: Generation and verification of a *Cgso* deletion strain in *C. graminicola*; Figure S2: Growth rates of *C. graminicola* strains; Figure S3: Generation of oval conidia *C. graminicola* wildtype and ΔCgso deletion mutant; Figure S4: Germling fusion rate of *C. graminicola* strains on water agar; Figure S5: *Zea mays* leaf infection; Figure S6: Quantification of empty and vacuolized hyphal compartments in *C. graminicola* hyphae; Figure S7: *C. graminicola* falcate conidiation on complex medium; Figure S8: Localization of the autophagy marker protein CgAtg8; Table S1: Oligonucleotides used in this study; Table S2: Plasmids used in this study; Table S3: *Colletotrichum graminicola* strains used in this study.

Funding: This work was funded by the Deutsche Forschungsgemeinschaft (Bonn-Bad Godesberg, project NO 1230/3-1 (447175909). We acknowledge support by the Open Access Publication Funds of the Göttingen University

Institutional Review Board Statement: Not applicable.

Informed Consent Statement: Not applicable.

Data Availability Statement: The data presented in this study are available on request from the corresponding author.

Acknowledgments: We are grateful to Gertrud Stahlhut and Gabriele Beyer for excellent technical assistance. We wish to thank Prof. Dr. Stefanie Pöggeler for critically reading the manuscript.

Conflicts of Interest: The authors declare no conflict of interest. The funders had no role in the design of the study, the conducted analyses, the interpretation of data, the writing of the manuscript, or in the decision to publish the results.

References

1. Bhunjun, C.S.; Phukhamsakda, C.; Jayawardena, R.S.; Jeewon, R.; Promputtha, I.; Hyde, K.D. Investigating species boundaries in *Colletotrichum*. *Fungal Diversity* **2021**, *107*, 107-127.
2. O'Connell, R.J.; Thon, M.R.; Hacquard, S.; Amyotte, S.G.; Kleemann, J.; Torres, M.F.; Damm, U.; Buiate, E.A.; Epstein, L.; Alkan, N. Lifestyle transitions in plant pathogenic *Colletotrichum* fungi deciphered by genome and transcriptome analyses. *Nature genetics* **2012**, *44*, 1060-1065.
3. Dean, R.; Van Kan, J.A.L.; Pretorius, Z.A.; Hammond-Kosack, K.E.; Di Pietro, A.; Spanu, P.D.; Rudd, J.J.; Dickman, M.; Kahmann, R.; Ellis, J. The Top 10 fungal pathogens in molecular plant pathology. *Molecular plant pathology* **2012**, *13*, 414-430.
4. Crouch, J.A.; Clarke, B.B.; White Jr, J.F.; Hillman, B.I. Systematic analysis of the falcate-spored graminicolous *Colletotrichum* and a description of six new species from warm-season grasses. *Mycologia* **2009**, *101*, 717-732.
5. Karunarathna, A.; Tibpromma, S.; Jayawardena, R.S.; Nanayakkara, C.; Asad, S.; Xu, J.; Hyde, K.D.; Karunarathna, S.C.; Stephenson, S.L.; Lumyong, S. Fungal Pathogens in Grasslands. *Frontiers in Cellular and Infection Microbiology* **2021**, *11*, 695087, doi:10.3389/fcimb.2021.695087.
6. Bergstrom, G.C.; Nicholson, R.L. The biology of corn anthracnose: knowledge to exploit for improved management. *Plant disease* **1999**, *83*, 596-608.
7. Sukno, S.A.; García, V.M.; Shaw, B.D.; Thon, M.R. Root infection and systemic colonization of maize by *Colletotrichum graminicola*. *Applied and environmental microbiology* **2008**, *74*, 823-832.
8. Perfect, S.E.; Hughes, H.B.; O'Connell, R.J.; Green, J.R. *Colletotrichum*: a model genus for studies on pathology and fungal–plant interactions. *Fungal genetics and Biology* **1999**, *27*, 186-198.
9. Frey, T.; Weldekidan, T.; Colbert, T.; Wolters, P.; Hawk, J. Fitness evaluation of *Rcg1*, a locus that confers resistance to *Colletotrichum graminicola* (Ces.) GW Wils. using near-isogenic maize hybrids. *Crop Science* **2011**, *51*, 1551-1563.
10. NISHIHARA, N. Two types of conidia of *Colletotrichum graminicola* (Ces.) GW Wils. formed on artificial media, and their pathogenicity. *Japanese Journal of Phytopathology* **1975**, *41*, 171-175.
11. Panaccione, D.G.; Vaillancourt, L.J.; Hanau, R.M. Conidial dimorphism in *Colletotrichum graminicola*. *Mycologia* **1989**, *81*, 876-883.
12. Frost, R. Seta Formation in *Colletotrichum* spp. *Nature* **1964**, *201*, 730-731.
13. Leite, B.; Nicholson, R.L. Mycosporine-alanine: A self-inhibitor of germination from the conidial mucilage of *Colletotrichum graminicola*. *Experimental mycology* **1992**, *16*, 76-86.

Preprints (www.preprints.org) | NOT PEER-REVIEWED | Posted: 17 March 2022 doi:10.20944/preprints202203.0242.v1

14. Nordzieke, D.E.; Sanken, A.; Antelo, L.; Raschke, A.; Deising, H.B.; Poggeler, S. Specialized infection strategies of falcate and oval conidia of *Colletotrichum graminicola*. *Fungal Genet Biol* **2019**, *133*, 103276, doi:10.1016/j.fgb.2019.103276.
15. Venard, C.; Vaillancourt, L. Colonization of fiber cells by *Colletotrichum graminicola* in wounded maize stalks. *Phytopathology* **2007**, *97*, 438-447.
16. Schunke, C.; Pöggeler, S.; Nordzieke, D.E. A 3D printed device for easy and reliable quantification of fungal chemotropic growth. *Front Microbiol* **2020**, *11*, 584525, doi:10.3389/fmicb.2020.584525.
17. Fleißner, A.; Herzog, S. Signal exchange and integration during self-fusion in filamentous fungi. In Proceedings of the Seminars in Cell & Developmental Biology, 2016; pp. 76-83.
18. Read, N.D.; Goryachev, A.B.; Lichius, A. The mechanistic basis of self-fusion between conidial anastomosis tubes during fungal colony initiation. *Fungal Biology Reviews* **2012**, *26*, 1-11.
19. Fischer, M.S.; Glass, N.L. Communicate and fuse: how filamentous fungi establish and maintain an interconnected mycelial network. *Frontiers in microbiology* **2019**, *10*, 619.
20. Fleißner, A.; Sarkar, S.; Jacobson, D.J.; Roca, M.G.; Read, N.D.; Glass, N.L. The so locus is required for vegetative cell fusion and postfertilization events in *Neurospora crassa*. *Eukaryotic Cell* **2005**, *4*, 920-930.
21. Fleißner, A.; Leeder, A.C.; Roca, M.G.; Read, N.D.; Glass, N.L. Oscillatory recruitment of signaling proteins to cell tips promotes coordinated behavior during cell fusion. *Proceedings of the National Academy of Sciences* **2009**, *106*, 19387-19392.
22. Goryachev, A.B.; Lichius, A.; Wright, G.D.; Read, N.D. Excitable behavior can explain the "ping-pong" mode of communication between cells using the same chemoattractant. *Bioessays* **2012**, *34*, 259-266.
23. Teichert, I.; Steffens, E.K.; Schnaß, N.; Fränzel, B.; Krisp, C.; Wolters, D.A.; Kück, U. PRO40 is a scaffold protein of the cell wall integrity pathway, linking the MAP kinase module to the upstream activator protein kinase C. *PLoS genetics* **2014**, *10*, e1004582.
24. Mehta, N.; Baghela, A. Quorum sensing-mediated inter-specific conidial anastomosis tube fusion between *Colletotrichum gloeosporioides* and *C. siamense*. *IMA fungus* **2021**, *12*, 1-17.
25. Roca, M.G.; Davide, L.C.; Davide, L.M.C.; Mendes-Costa, M.C.; Schwan, R.F.; Wheals, A.E. Conidial anastomosis fusion between *Colletotrichum* species. *Mycological Research* **2004**, *108*, 1320-1326.
26. Forgey, W.M.; Blanco, M.H.; Loegering, W.Q. Differences in pathological capabilities and host specificity of *Colletotrichum graminicola* on *Zea mays*. *Plant Disease Reporter (USA)* **1978**, 573–576.
27. Sambrook, J.; Fritsch, E.; Maniatis, T., (Eds.) *Molecular Cloning: A Laboratory Manual*. Cold Spring Harbor Laboratory Press, Cold Spring Harbor, NY, USA: 2001.
28. Bloemendal, S.; Bernhards, Y.; Bartho, K.; Dettmann, A.; Voigt, O.; Teichert, I.; Seiler, S.; Wolters, D.A.; Pöggeler, S.; Kück, U. A homologue of the human STRIPAK complex controls sexual development in fungi. *Molecular microbiology* **2012**, *84*, 310-323.
29. Klix, V.; Nowrousian, M.; Ringelberg, C.; Loros, J.; Dunlap, J.; Pöggeler, S. Functional characterization of MAT1-1-specific mating-type genes in the homothallic ascomycete *Sordaria macrospora* provides new insights into essential and nonessential sexual regulators. *Eukaryotic cell* **2010**, *9*, 894-905.
30. Pöggeler, S.; Masloff, S.; Hoff, B.; Mayrhofer, S.; Kück, U. Versatile EGFP reporter plasmids for cellular localization of recombinant gene products in filamentous fungi. *Current genetics* **2003**, *43*, 54-61.
31. Groth, A.; Schunke, C.; Reschka, E.J.; Pöggeler, S.; Nordzieke, D.E. Tracking fungal growth: Establishment of Arp1 as a marker for polarity establishment and active hyphal growth in filamentous ascomycetes. *Journal of Fungi* **2021**, *7*, 580.
32. Schindelin, J.; Arganda-Carreras, I.; Frise, E.; Kaynig, V.; Longair, M.; Pietzsch, T.; Preibisch, S.; Rueden, C.; Saalfeld, S.; Schmid, B.; et al. Fiji: an open-source platform for biological-image analysis *Nat Methods* **2019**, *9*, 676-682, doi:10.1038/nmeth.2019.
33. Ruxton, G.D. The unequal variance t-test is an underused alternative to Student's t-test and the Mann–Whitney U test. *Behavioral Ecology* **2006**, *17*, 688-690.
34. Wen, X.; Klionsky, D.J. An overview of macroautophagy in yeast. *Journal of molecular biology* **2016**, *428*, 1681-1699.
35. Voigt, O.; Pöggeler, S. Autophagy genes *Smatg8* and *Smatg4* are required for fruiting-body development, vegetative growth and ascospore germination in the filamentous ascomycete *Sordaria macrospora*. *Autophagy* **2013**, *9*, 33-49.
36. Felkner, I.C.; Wyss, O. A substance produced by competent *Bacillus cereus* 569 cells that affects transformability. *Biochemical and biophysical research communications* **1964**, *16*, 94-99.
37. Tomasz, A.; Hotchkiss, R.D. Regulation of the transformability of pneumococcal cultures by macromolecular cell products. *Proceedings of the National Academy of Sciences of the United States of America* **1964**, *51*, 480.
38. Hogan, D.A. Talking to themselves: autoregulation and quorum sensing in fungi. *Eukaryotic cell* **2006**, *5*, 613-619.
39. Barriuso, J.; Hogan, D.A.; Keshavarz, T.; Martínez, M.J. Role of quorum sensing and chemical communication in fungal biotechnology and pathogenesis. *FEMS microbiology reviews* **2018**, *42*, 627-638.
40. Padder, S.A.; Prasad, R.; Shah, A.H. Quorum sensing: a less known mode of communication among fungi. *Microbiological research* **2018**, *210*, 51-58.
41. Roca, G.M.; Read, N.D.; Wheals, A.E. Conidial anastomosis tubes in filamentous fungi. *FEMS microbiology letters* **2005**, *249*, 191-198.
42. Mehta, N.; Patil, R.; Baghela, A. Differential physiological prerequisites and gene expression profiles of conidial anastomosis tube and germ tube formation in *Colletotrichum gloeosporioides*. *Journal of Fungi* **2021**, *7*, 509.
43. Kurian, S.M.; Di Pietro, A.; Read, N.D. Live-cell imaging of conidial anastomosis tube fusion during colony initiation in *Fusarium oxysporum*. *PLoS One* **2018**, *13*, e0195634.
44. Miller MB; BL, B. Quorum sensing in bacteria. *Annu Rev Microbiol* **2001**, *55*, 165–199.

Preprints (www.preprints.org) | NOT PEER-REVIEWED | Posted: 17 March 2022 doi:10.20944/preprints202203.0242.v1

45. Sanogo, S.; Stevenson, R.; Pennypacker, S. Appressorium formation and tomato fruit infection by *Colletotrichum coccodes*. *Plant disease* **2003**, *87*, 336-340.
46. Vitale, S.; Di Pietro, A.; Turrà, D. Autocrine pheromone signalling regulates community behaviour in the fungal pathogen *Fusarium oxysporum*. *Nature microbiology* **2019**, *4*, 1443-1449.
47. Zhu, X.-M.; Li, L.; Wu, M.; Liang, S.; Shi, H.-B.; Liu, X.-H.; Lin, F.-C. Current opinions on autophagy in pathogenicity of fungi. *Virulence* **2019**, *10*, 481-489.
48. Kim, J.; Huang, W.-P.; Klionsky, D.J. Membrane recruitment of Aut7p in the autophagy and cytoplasm to vacuole targeting pathways requires Aut1p, Aut2p, and the autophagy conjugation complex. *The Journal of cell biology* **2001**, *152*, 51-64.
49. Suzuki, K.; Kirisako, T.; Kamada, Y.; Mizushima, N.; Noda, T.; Ohsumi, Y. The pre-autophagosomal structure organized by concerted functions of APG genes is essential for autophagosome formation. *The EMBO journal* **2001**, *20*, 5971-5981.
50. Suzuki, K.; Ohsumi, Y. Molecular machinery of autophagosome formation in yeast, *Saccharomyces cerevisiae*. *FEBS letters* **2007**, *581*, 2156-2161.
51. Levine, B.; Yuan, J. Autophagy in cell death: an innocent convict? *The Journal of clinical investigation* **2005**, *115*, 2679-2688.
52. Teter, S.A.; Eggerton, K.P.; Scott, S.V.; Kim, J.; Fischer, A.M.; Klionsky, D.J. Degradation of lipid vesicles in the yeast vacuole requires function of Cvt17, a putative lipase. *Journal of Biological Chemistry* **2001**, *276*, 2083-2087.
53. Epple, U.D.; Suriapranata, I.; Eskelinen, E.-L.; Thumm, M. Aut5/Cvt17p, a putative lipase essential for disintegration of autophagic bodies inside the vacuole. *Journal of bacteriology* **2001**, *183*, 5942-5955.
54. Voigt, O.; Pöggeler, S. Self-eating to grow and kill: autophagy in filamentous ascomycetes. *Applied microbiology and biotechnology* **2013**, *97*, 9277-9290.
55. Inoue, Y.; Klionsky, D.J. Regulation of macroautophagy in *Saccharomyces cerevisiae*. In Proceedings of the Seminars in cell & developmental biology, 2010; pp. 664-670.
56. Geng, J.; Klionsky, D.J. The Atg8 and Atg12 ubiquitin-like conjugation systems in macroautophagy. *EMBO reports* **2008**, *9*, 859-864.
57. Kirisako, T.; Ichimura, Y.; Okada, H.; Kabeya, Y.; Mizushima, N.; Yoshimori, T.; Ohsumi, M.; Takao, T.; Noda, T.; Ohsumi, Y. The reversible modification regulates the membrane-binding state of Apg8/Aut7 essential for autophagy and the cytoplasm to vacuole targeting pathway. *The Journal of cell biology* **2000**, *151*, 263-276.
58. Liu, Z.-M.; Kolattukudy, P.E. Early expression of the calmodulin gene, which precedes appressorium formation in *Magnaporthe grisea*, is inhibited by self-inhibitors and requires surface attachment. *Journal of Bacteriology* **1999**, *181*, 3571-3577.
59. Teichert, I.; Pöggeler, S.; Nowrousian, M. *Sordaria macrospora*: 25 years as a model organism for studying the molecular mechanisms of fruiting body development. *Applied Microbiology Biotechnology* **2020**, *104*, 3691-3704.
60. Deng, Y.Z.; Ramos-Pamplona, M.; Naqvi, N.I. Autophagy-assisted glycogen catabolism regulates asexual differentiation in *Magnaporthe oryzae*. *Autophagy* **2009**, *5*, 33-43.
61. Veneault-Fourrey, C.; Barooah, M.; Egan, M.; Wakley, G.; Talbot, N.J. Autophagic fungal cell death is necessary for infection by the rice blast fungus. *Science* **2006**, *312*, 580-583.
62. Kershaw, M.J.; Talbot, N.J. Genome-wide functional analysis reveals that infection-associated fungal autophagy is necessary for rice blast disease. *Proceedings of the National Academy of Sciences* **2009**, *106*, 15967-15972.
63. Kikuma, T.; Arioka, M.; Kitamoto, K. Autophagy during conidiation and conidial germination in filamentous fungi. *Autophagy* **2007**, *3*, 128-129.
64. Nitsche, B.M.; Burggraaf-van Welzen, A.-M.; Lamers, G.; Meyer, V.; Ram, A.F. Autophagy promotes survival in aging submerged cultures of the filamentous fungus *Aspergillus niger*. *Applied microbiology and biotechnology* **2013**, *97*, 8205-8218.
65. Kikuma, T.; Ohneda, M.; Arioka, M.; Kitamoto, K. Functional analysis of the *ATG8* homologue Ao*atg8* and role of autophagy in differentiation and germination in *Aspergillus oryzae*. *Eukaryotic cell* **2006**, *5*, 1328-1336.
66. Asakura, M.; Ninomiya, S.; Sugimoto, M.; Oku, M.; Yamashita, S.; Okuno, T.; Sakai, Y.; Takano, Y. Atg26-mediated pexophagy is required for host invasion by the plant pathogenic fungus *Colletotrichum orbiculare*. *The Plant Cell* **2009**, *21*, 1291-1304.
67. Josefsen, L.; Droce, A.; Sondergaard, T.E.; Sørensen, J.L.; Bormann, J.; Schäfer, W.; Giese, H.; Olsson, S. Autophagy provides nutrients for nonassimilating fungal structures and is necessary for plant colonization but not for infection in the necrotrophic plant pathogen *Fusarium graminearum*. *Autophagy* **2012**, *8*, 326-337.
68. Meng, S.; Xiong, M.; Jagernath, J.S.; Wang, C.; Qiu, J.; Shi, H.; Kou, Y. UvAtg8-mediated autophagy regulates fungal growth, stress responses, conidiation, and pathogenesis in *Ustilaginoidea virens*. *Rice* **2020**, *13*, 1-13.
69. Roca, M.G.; Davide, L.C.; Mendes-Costa, M.C.; Wheals, A. Conidial anastomosis tubes in *Colletotrichum*. *Fungal Genetics and Biology* **2003**, *40*, 138-145.
70. Bloemendal, S.; Lord, K.M.; Rech, C.; Hoff, B.; Engh, I.; Read, N.D.; Kück, U. A mutant defective in sexual development produces aseptate ascogonia. *Eukaryotic cell* **2010**, *9*, 1856-1866.
71. Dirschnabel, D.E.; Nowrousian, M.; Cano-Domínguez, N.; Aguirre, J.; Teichert, I.; Kück, U. New insights into the roles of NADPH oxidases in sexual development and ascospore germination in *Sordaria macrospora*. *Genetics* **2014**, *196*, 729-744.
72. Kück, U. A *Sordaria macrospora* mutant lacking the *leu1* gene shows a developmental arrest during fruiting body formation. *Molecular Genetics and Genomics* **2005**, *274*, 307-315.
73. Masloff, S.; Pöggeler, S.; Kück, U. The *pro1*$^{+}$ gene from *Sordaria macrospora* encodes a C_6 zinc finger transcription factor required for fruiting body development. *Genetics* **1999**, *152*, 191-199.

Preprints (www.preprints.org) | NOT PEER-REVIEWED | Posted: 17 March 2022 doi:10.20944/preprints202203.0242.v1

74. Nowrousian, M.; Frank, S.; Koers, S.; Strauch, P.; Weitner, T.; Ringelberg, C.; Dunlap, J.C.; Loros, J.J.; Kück, U. The novel ER membrane protein PRO41 is essential for sexual development in the filamentous fungus *Sordaria macrospora*. *Molecular microbiology* **2007**, *64*, 923-937.
75. Nowrousian, M.; Masloff, S.; Pöggeler, S.; Kück, U. Cell differentiation during sexual development of the fungus *Sordaria macrospora* requires ATP citrate lyase activity. *Molecular and cellular biology* **1999**, *19*, 450-460.
76. Nowrousian, M.; Teichert, I.; Masloff, S.; Kück, U. Whole-genome sequencing of *Sordaria macrospora* mutants identifies developmental genes. *G3: Genes| Genomes| Genetics* **2012**, *2*, 261-270.
77. Pöggeler, S.; Kück, U. A WD40 repeat protein regulates fungal cell differentiation and can be replaced functionally by the mammalian homologue striatin. *Eukaryotic cell* **2004**, *3*, 232-240.
78. Bernhards, Y.; Pöggeler, S. The phocein homologue SmMOB3 is essential for vegetative cell fusion and sexual development in the filamentous ascomycete *Sordaria macrospora*. *Current genetics* **2011**, *57*, 133-149.
79. Nordzieke, S.; Zobel, T.; Fränzel, B.; Wolters, D.A.; Kück, U.; Teichert, I. A fungal sarcolemmal membrane-associated protein (SLMAP) homolog plays a fundamental role in development and localizes to the nuclear envelope, endoplasmic reticulum, and mitochondria. *Eukaryotic cell* **2015**, *14*, 345-358.
80. Werner, A.; Herzog, B.; Frey, S.; Pöggeler, S. Autophagy-associated protein SmATG12 is required for fruiting-body formation in the filamentous ascomycete *Sordaria macrospora*. *PLoS One* **2016**, *11*, e0157960.